Available online at www.sciencedirect.com
ScienceDirect
Russian Geology and Geophysics 51 (2010) 507–520
RUSSIAN GEOLOGY AND GEOPHYSICS
www.elsevier.com/locate/rgg

Physico-chemical parameters of Neoproterozoic and Early Cambrian plume magmatism in the Paleo-Asian ocean (*data on melt inclusions*)

V.A. Simonov *, I.Yu. Safonova, S.V. Kovyazin, A.V. Kotlyarov

V.S. Sobolev Institute of Geology and Mineralogy, Siberian Branch of the Russian Academy of Sciences, prosp. Akad. Koptyuga 3, Novosibirsk, 630090, Russia

Received 20 April 2009

Abstract

The paper presents new data on physico-chemical parameters of the Neoproterozoic–Early Cambrian plume magmatism in the Paleo-Asian Ocean. The data on clinopyroxenes show the plume-related plateaubasalt magmatic systems of the Katun' paleoseamounts, which interacted with mid-ocean ridge (MOR) magmas. The Kurai paleoseamount consists mainly of plateaubasalt systems, and the Agardag ophiolites represent products of OIB–type "hot-spot" within-plate magmatism. Our study of inclusions showed that the melts of the Katun' and Kurai paleoseamounts crystallized at lower temperatures (1130–1190 °C) compared to the Agardag ophiolites (1210–1255 °C). The petrochemical analysis of the melt inclusions showed that the Katun' and Kurai magmatic systems are different from the Mg- and Ti-richer melts of the Agardag ophiolites: the former are similar to the magmas of the Nauru Basin and Ontong Java Plateau (western Pacific), whereas the latter possess geochemical affinities to OIB-type magmatism. The rare-element compositions of the melts of the Katun' and Kurai paleoseamounts correspond to those of the Ontong Java Plateau and Nauru Basin lavas. The numerically simulated parameters of the Katun' paleoseamount primary magmas agree with the data on the magmatic systems of the Siberian Platform and Ontong Java Plateau. For the Kurai paleoseamount, the simulated results suggest interaction of deep-seated OIB-type magmatic systems with MOR ones. The Agardag ophiolites were formed in relation to mantle plume activity at the initial stages of paleo-oceanic complexes formation.
© 2010, V.S. Sobolev IGM, Siberian Branch of the RAS. Published by Elsevier B.V. All rights reserved.

Keywords: physico-chemical parameters; plume magmatism; melt inclusions; Paleo-Asian ocean

Introduction

In recent years, fragments of oceanic plateaus, seamounts, and oceanic islands related to plume magmatism in the Paleo-Asian ocean have been found in Asian fold belts. Those fragments are not oceanic basalts only, but also occur as large siliceous-carbonate complexes, which are difficult to distinguish from similar sedimentary rocks of other genesis. Since oceanic islands and seamounts in modern oceans are comparable in area and volume with island arcs, the recognition of such objects among Paleo-Asian oceanic structures and their study are of crucial importance. Due to active research in this field, volcanogenic-siliceous-carbonate-terrigenous units of paleoseamounts have been discovered in Central Asia (Dobretsov, 2003; Dobretsov et al., 2004, 2005; Gordienko and Filimonov, 2005; Gordienko et al., 2003, 2007; Safonova, 2009; Safonova et al., 2004, 2009). These findings considerably change the available ideas about stratigraphy, tectonics, and paleogeography of Altai–Sayan region.

Based on the results of Gorny Altai, the carbonate-siliceous and volcanogenic complexes of the Neoproterozoic Baratal and Early Cambrian Katun' paleo-oceanic islands were described (Dobretsov et al., 2004). The data on the geochemistry of basalts of the Kurai and Katun' paleoseamounts (Gorny Altai) are indicative of their formation in relation to mantle plumes (Safonova, 2008; Safonova et al., 2008). The investigations of paleo-oceanic structures in the Chara zone (eastern Kazakhstan) revealed fragments of Devonian–Early Cambrian paleo-oceanic islands with OIB-type magmatism (Dobretsov, 2003; Safonova et al., 2004, 2009). Study of the composition of basaltic rocks from the Zasur'ya Formation (northwestern Altai) showed the formation of OIB-type magmatic systems in the Late Cambrian and Early Ordovician (Safonova et al., 2004, 2009).

Recently, the presence of structure-lithologic complexes of ensimatic island arc, guyots (seamounts), and fore-arc and

* Corresponding author.
E-mail address: simonov@uiggm.nsc.ru (V.A. Simonov)

1068-7971/$ - see front matter © 2010, V.S. Sabolev IGM, Siberian Branch of the RAS. Published by Elsevier B.V. All rights reserved.
doi:10.1016/j.rgg.2010.04.004

back-arc paleobasins has been established in the Dzhida zone of the Paleo-Asian ocean. In the position and structure the Dzhida zone guyots are similar to the Gorny Altai paleoseamounts (Gordienko et al., 2003, 2007; Gordienko and Filimonov, 2005).

Complex studies permitted Dobertsov et al. (2005) to establish the parameters of basalt petrogenesis and refine the paleogeodynamic setting of formation of the Kurai paleoseamount (Gorny Altai). Recently, we have obtained the first data on melt inclusions in clinopyroxenes of the Katun' paleoseamount in Gorny Altai (Simonov et al., 2008).

Despite the crucial significance of the structures of ancient oceanic plateaus, seamounts, and oceanic islands and the great interest to them, many questions of their structure, composition, and formation conditions are still debatable. The reliable identification of these structures somewhat similar to other oceanic and island-arc complexes is problematic, mainly because of the great alteration of rocks. The physico-chemical conditions of magmatic processes, parameters of primary mantle melts, and effect of mantle plumes are still unclear. Complex geological, mineralogical, and geochemical studies and analysis of melt inclusions in minerals in comparison with the objects in modern oceanic regions are the best way to solve the above problems.

In this work we present the results of investigations (mainly, by studying primary magmatogene minerals and melt inclusions) of the conditions of plume magmatic systems that formed complexes of Paleo-Asian oceanic plateaus, seamounts, and islands in the Neoproterozoic and Early Cambrian.

Methods and approaches

In the course of investigations, special attention was given to study of preserved magmatogene minerals and melt inclusions bearing direct information on ancient magmatic systems. The rocks sampled during our expedition works in different regions of the Altai–Sayan area were studied mainly at the V.S. Sobolev Institute of Geology and Mineralogy, Novosibirsk. Mineral compositions were examined on a Camebax Micro probe. High-temperature experiments on melt inclusions were carried out on thermal microstage with inert medium (Sobolev and Slutskii, 1984), following known techniques (Simonov, 1993; Sobolev and Danyushevsky, 1994; Sobolev et al, 2009). The homogenized inclusions quenched to glass were analyzed on a Camebax Micro probe at the V.S. Sobolev Institute of Geology and Mineralogy, Novosibirsk. The contents of trace and rare-earth elements and water in the inclusions were determined by secondary-ion mass spectrometry on an IMS-4f microprobe at the Institute of Microelectronics, Yaroslavl, following the technique proposed by Sobolev (1996).

Investigations of the Paleo-Asian oceanic structures were based on a comparative analysis of the data obtained and the results of study of melt inclusions in minerals from the Mid-Atlantic Ridge (Simonov et al., 1999), oceanic Bouvet Island (southern Atlantic Ocean) (Simonov et al., 1996, 2000), underwater Ontong Java Plateau, and Nauru Basin in the Pacific (Simonov et al., 2004, 2005).

Geological outline

During the long-standing expedition works in Central Asia, many paleo-oceanic structures of Neoproterozoic and Early Cambrian ages were studied in detail. We examined a great number of samples from different complexes of the Paleo-Asian ocean that have plume geochemistry but succeeded in obtaining data on primary magmatogene minerals and melt inclusions for only three objects localized in Gorny Altai (Katun' and Kurai paleoseamounts) and Tuva (ophiolites of the Agardag zone, southern Tuva) (Fig. 1). The geology, petrochemistry, and geochemistry of rocks from these reference associations were considered in detail in our previous papers (Dobretsov et al., 2004, 2005; Safonova, 2008; Safonova et al., 2009). Therefore, in this paper we characterize the basaltic series in brief and focus the main attention on study of clinopyroxenes and melt inclusions.

The Katun' paleoseamount. In the Katun' River area (from the Ustyuba River mouth to the Edigan River), the paleoseamount includes three rock complexes. The complex of type 1 is composed of dark gray carbonaceous limestones, black silicilites, clayey and clay-siliceous shales, dolomites, and scarce thin basalt flows. Sedimentary rocks are predominant in the section above volcanics. The complex of type 2 is formed by high- and low-Ti tholeiitic and alkali basalts and their clastic lavas and lava clastites with siliceous, carbonate, and clayey deposits. The complex of type 3 consists of laminated limestones and dolomites with tuff interbeds. All these tectonic plates are fragments of a paleo-oceanic island. The type 1 complex includes mainly slope rock facies, and

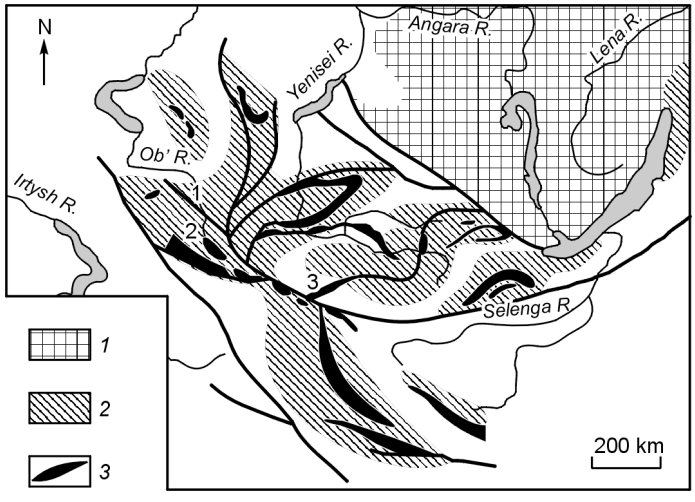

Fig. 1. Localization of the studied Paleo-Asian oceanic structures. *1*, Siberian Platform; *2*, folded structures; *3*, zones of paleo-oceanic structures. Numerals mark the positions of the Katun' (1) and Kurai (2) paleoseamounts and Agardag ophiolites (3).

the type 2 and type 3 complexes, the rocks of the basement of the oceanic island and its carbonate cap.

The Early Cambrian volcanics of the Katun' paleoseamount are thin flows of tholeiitic basalts (N-MORB) and large volcanic buildings composed of alkali basalts corresponding in composition to within-plate plume OIB with high contents of Ti, Nb, and LREE (Dobretsov et al., 2004; Safonova, 2008).

Most of the ancient basaltoids of the Katun' paleoseamount were significantly altered, and primary minerals were replaced by secondary parageneses. Clinopyroxene with occasional melt inclusions (MIs) is often preserved. The most informative data on magmatic minerals and inclusions were obtained for a lava flow sampled in the Cheposh Village region (northern Gorny Altai). It is composed of altered basalts with a quenched microlithic groundmass and small (0.2–1 mm) clinopyroxene phenocrysts (sample Kat-55-07). In geochemistry the rock corresponds to within-plate oceanic plume basalts (Safonova et al., 2009).

The Kurai paleoseamount. North of the Kurai Village (Gorny Altai), basalts compose a fragment of paleoseamount. There are primary relationships between the basalts and the carbonate "cap" and slope facies deposits as well as between the basalts of the oceanic bottom and the volcanosedimentary rocks of the paleoseamount basement (Dobretsov et al., 2004; Safonova et al., 2008). The basaltic strata are formed by pillow lavas and dikes of pyroxene and plagioclase porphyrites, aphyric basalts, and diabases. The Late Neoproterozoic age of basalts is estimated from the age of the associated limestones—598 Ma (Uchio et al., 2004).

The Kurai paleoseamount includes volcanogenic, volcanosedimentary, and sedimentary strata. The *volcanogenic strata* (magmatic basis of the paleoisland) are composed mainly of pillow lavas of plagioclase and pyroxene-plagioclase basaltic porphyrites. Also, rare interbeds and lenses of marbleized limestones and dolomites and, more seldom, siliceous rocks and volcanomict sandstones occur. The *volcanosedimentary strata* (slope facies) are formed by laminated and massive limestones, siliceous rocks, pillow lavas, and volcanoclastites alternating with chloritized clayey rocks and volcanomict sandstones. The sedimentary rocks show features evidencing their formation on the slopes of a volcanic building, namely, consedimentatiton folds, brecciation, and rock beds of varying thickness. The *sedimentary strata* (carbonate "cap") are composed of carbonate and siliceous rocks. The carbonate rocks are gray massive and laminated limestones and carbonate breccias.

The basalts of the Kurai paleoseamount are subdivided into Ti, Nb, LREE-depleted, transitional, and enriched varieties. The Ti, Nb, LREE-depleted basalts are similar in composition to N-MORB and are associated with fine-laminated siliceous deposits. The transitional and Ti, Nb, LREE-enriched varieties are similar to the Pacific within-plate basalts and are associated with the carbonate-siliceous deposits of slope facies and the limestones of the carbonate "cap" of oceanic rises (plateaus and seamounts) (Safonova et al., 2008).

Investigations of a representative collection of rocks from the Kurai paleoseamount showed that basaltic and diabase porphyrites sampled from dikes (S-80A-04) and lavas (S-79-04, S-117V-05) in the Kurai Village region (Karatyurgun site) are the most promising for analysis of clinopyroxenes and hosted inclusions. These basalts are the most similar in petrochemistry and geochemistry to rocks of the Pacific within-plate oceanic plateaus and islands (Dobretsov et al., 2004; Safonova et al., 2008).

The Agardag ophiolites. In the Neoproterozoic (570 Ma (Kozakov et al., 2003)) Agardag ophiolite zone stretching in southern Tuva for more than 120 km, four main sites are recognized in passing from west to east, which contain different fragments of paleo-oceanic crust: (1) Agardag (predominance of ultrabasites of the ophiolite basement); (2) Karashat (dunite-wehrlite-pyroxenite complex + gabbros + dike series); (3) Tes-Khem (dikes + lavas); and (4) Chon-Sair (gabbros + dike complex). The igneous complexes of the Tes-Khem site, formed with the participation of plume magmatic systems (Dobretsov et al., 2005), are of paramount interest.

The Tes-Khem site is located in the watershed of the Tes-Khem and Terektig-Sair Rivers. The geology of this site was partly considered earlier (Gibsher and Terleev, 1988; Izokh et al., 1988; Tarasko et al., 2005). We have recognized four main sheets: a gabbro-dike complex similar to that at the Karashat site, carbonate-terrigenous sheet with a series of dikes (making up to 50% and more of the rock volume), serpentinite melange zone with dike blocks, and volcanosedimentary sheet with lava flows and dikes.

Geochemical studies showed that mainly two magmatic systems were responsible for the formation of the igneous rocks of the Tes-Khem site. One, which produced a gabbro-dike complex, was intimately related to the evolution of the layered ophiolite gabbro-ultrabasite associations of the Karashat massif. The evolution of the second proceeded with the formation of spreading dike series and lavas in effusive-sedimentary strata.

The lavas of the volcanic-sedimentary strata have high contents of TiO_2 (up to 3.1 wt.%). In the TiO_2–K_2O and TiO_2–FeO/MgO plots they are intimately associated with OIB, which evidences the enrichment of their source with these components and the influence of mantle plume. On the correlation diagrams, the fields of dike series rocks overlap with the wide field of lavas. This indicates that the dikes and lavas of the Tes-Khem site are comagmatic. The ratios of trace elements (Y, Zr, Nb) in the dikes and lavas also point to a plume source (Dobretsov et al., 2005). In general, these dikes and lavas are geochemically similar to the high-TiO_2 tholeiitic dike complexes of the Tehama Asir ophiolites (Red Sea region), whose formation was related to rifting, the opening of the Red Sea, and the formation of new oceanic crust as a result of spreading (Coleman et al., 1979).

Despite the great number of dike and lava samples collected at the Tes-Khem site, we succeeded in finding preserved clinopyroxenes with melt inclusions only in porphyrites from the pillow lavas (S-25N-99) of the volcanosedimentary strata on the right bank of the Tes-Khem River.

Clinopyroxenes

Clinopyroxenes are good indicators of various parameters of magmatic systems as their compositions reflect the main geochemical properties of the melts. We analyzed clinopyroxenes and their hosted melt inclusions (MIs) in all three objects under study (Katun' and Kurai paleoseamounts in Gorny Altai and Agardag ophiolites in southern Tuva). Table 1 presents clinopyroxene compositions. The most of the studied clinopyroxenes hosting MIs occurs as 1–2 mm nonzoned grains. This made us impossible to follow the evolution of their characteristics, which are usually manifested in phenocryst zoning.

In the proportion of En, Wo, and Fs the pyroxenes from the studied Gorny Altai paleo-oceanic rock complexes correspond to augites, whereas the minerals from the effusive rocks of the Agardag ophiolites are richer in Ca and are referred to as diopsides. Clinopyroxenes from the Kurai paleoseamount porphyrites contain more FeO than those from the Katun' paleosemount.

On the $SiO_2/100$–TiO_2–Na_2O diagram, the clinopyroxenes from the Kurai paleoseamount and Agardag ophiolites are localized mainly in the fields of minerals from within-plate oceanic subalkalic basalts. The former are similar to Ti-poorer pyroxenes from MOR tholeiites, whereas the latter, richer in Ti, partly fall into the field of within-plate oceanic alkaline rocks. The clinopyroxenes from the Katun' paleoseamount are localized mainly in the field of minerals from MOR tholeiites (Fig. 2). The observed differences are confirmed by the Ti–(Ca + Na) diagram, where the Katun' paleoseamount clinopyroxenes are confined mainly to the field of normal-alkalinity rocks, whereas those from the Kurai paleoseamount and Agardag ophiolites fall mainly into the field of alkaline rocks.

On the TiO_2–FeO diagram, the Katun' paleoseamount clinopyroxenes form a trend running from minimum contents of these components (TiO_2 = 0.4, FeO = 4.8 wt.%, field of minerals from MORB) to high ones (TiO_2 = 0.8, FeO = 8.4 wt.%; field of minerals from plateaubasalts). The Kurai paleoseamount clinopyroxenes totally fall into the field of pyroxenes from the effusive rocks of the Siberian Platform. The high contents of TiO_2 (up to 1.3–2 wt.%) and medium ones of FeO (up to 6.3–7.9 wt.%) in the clinopyroxenes from lavas of the Agardag ophiolites make them similar to the minerals of within-plate plume OIB (Fig. 3).

The Katun' paleoseamount clinopyroxenes show significant variations in Cr contents, which is, most likely, related to the rapid crystallization of micrograins (smaller than 1 mm) in contrast to the formation of larger (~1–2 mm) phenocrysts in more stable conditions at the Kurai paleoseamount.

Though we performed much research work, we succeeded in obtaining representative data on trace and rare-earth elements only for the clinopyroxenes from the Kurai paleoseamount (Table 2).

Analysis of the REE patterns of clinopyroxenes from the Kurai paleoseamount showed that all of them are enriched in REE as compared with similar minerals of other paleo-oceanic igneous complexes (ophiolites of the Arctic Urals and Troodos, Cyprus; Table 2), whose REE contents are close to or slightly higher than those in chondrite (Batanova et al., 1996; Simonov et al., 2000). A common property of the studied clinopyroxenes is a significant depletion in LREE (La, Ce, Nd) relative to normal and heavy REE (Fig. 4). This is expressed as the low $(La/Yb)_n$ values (0.07–0.22) and the positive slope of the REE patterns. A similar LREE depletion was earlier established in pyroxenes from other intrusive and effusive ophiolite complexes: Samail in Oman (Pallister and Knight, 1981), Troodos on Cyprus (Batanova and Savelieva,

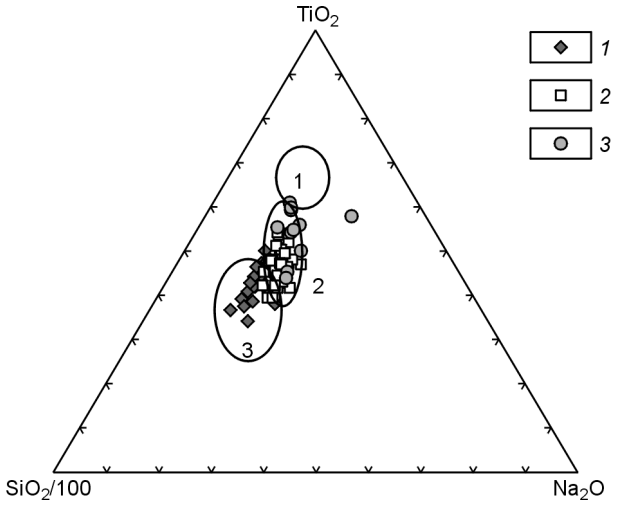

Fig. 2. $SiO_2/100$–TiO_2–Na_2O diagram for clinopyroxenes. *1–3*, clinopyroxenes from the rocks of the Katun' (*1*) and Kurai (*2*) paleoseamounts and Agardag ophiolites (*3*). Fields of clinopyroxenes from within-plate oceanic alkali (1) and subalkalic (2) basalts and tholeiitic basalts of MOR rifts (3) are shown. Constructed on the basis of our new data and those borrowed from Tsameryan et al. (1991).

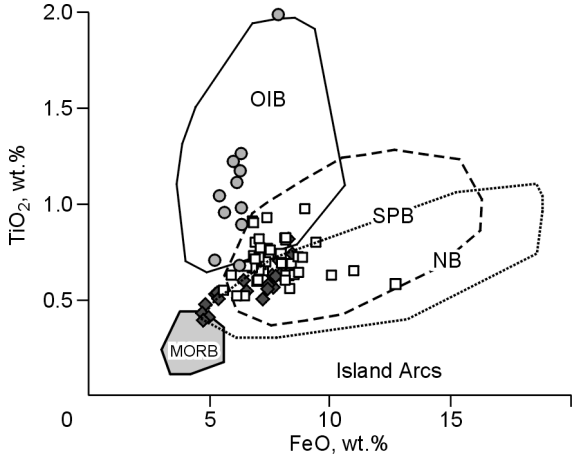

Fig. 3. TiO_2–FeO diagram for clinopyroxenes. Fields of clinopyroxenes from MORB, within-plate OIB, basalts of the Siberian Platform (SPB), basalts of the Nauru Basin (Ontong Java Plateau) (NB), and island-arc basalts (Island Arcs) are shown. Constructed on the basis of our new and earlier (Simonov et al., 2005) data. Designations follow Fig. 2.

Table 1. Representative analyses of clinopyroxenes (wt.%)

No.	Run	SiO_2	TiO_2	Al_2O_3	Cr_2O_3	FeO	MnO	MgO	CaO	Na_2O	K_2O	Total	MgO#
1	1	52.44	0.54	2.37	0.14	6.52	0.23	16.97	19.90	0.22	0.00	99.33	82.26
2	9	51.77	0.60	3.00	0.31	6.39	0.15	16.27	19.99	0.24	0.02	98.74	81.94
3	11	53.12	0.46	2.13	0.19	4.79	0.11	17.39	20.54	0.19	0.01	98.93	86.61
4	17	52.86	0.40	1.98	0.23	4.99	0.09	17.70	20.79	0.17	0.01	99.22	86.34
5	19	50.80	0.63	2.75	0.11	7.78	0.21	16.33	19.71	0.28	0.01	98.60	78.90
6	24	50.85	0.70	2.92	0.09	7.88	0.17	16.08	19.73	0.25	0.01	98.69	78.43
7	26	50.88	0.62	2.71	0.11	7.59	0.19	16.45	19.66	0.22	0.00	98.43	79.43
8	27	52.21	0.55	2.42	0.06	7.42	0.21	16.73	19.10	0.22	0.00	98.92	80.07
9	28	52.48	0.56	2.45	0.03	7.62	0.22	16.36	19.17	0.26	0.00	99.15	79.28
10	33	51.51	0.74	2.84	0.01	8.42	0.17	16.50	18.31	0.23	0.00	98.73	77.74
11	34	51.93	0.63	2.68	0.05	7.93	0.22	16.74	18.46	0.21	0.01	98.87	79.00
12	35	51.93	0.57	2.42	0.10	7.42	0.20	16.87	19.26	0.21	0.00	98.99	80.20
13	1	51.85	0.69	2.52	0.19	7.13	0.18	15.85	20.66	0.28	0.00	99.35	79.84
14	7	51.01	0.80	3.45	0.28	6.89	0.17	15.66	20.61	0.29	0.01	99.17	80.20
15	10	52.04	0.69	2.59	0.22	6.86	0.17	16.32	20.82	0.27	0.01	99.99	80.91
16	46	51.41	0.63	2.28	0.07	8.30	0.25	17.11	19.54	0.36	0.01	99.96	78.60
17	49	51.65	0.69	2.36	0.06	8.02	0.20	16.55	19.98	0.31	0.00	99.81	78.62
18	59	51.15	0.70	3.10	0.22	7.33	0.20	16.22	20.68	0.31	0.00	99.90	79.77
19	64	50.74	0.81	3.29	0.19	8.19	0.21	15.59	20.48	0.40	0.00	99.90	77.23
20	70	50.38	0.66	2.87	0.24	7.06	0.18	16.51	20.82	0.31	0.00	99.03	80.65
21	4	51.53	0.82	2.88	0.19	7.05	0.17	15.76	20.61	0.30	0.03	99.34	79.93
22	11	51.46	0.93	3.17	0.11	7.39	0.19	15.67	20.78	0.26	0.00	99.96	79.07
23	7	52.24	0.52	2.39	0.40	6.45	0.17	17.00	20.28	0.28	0.00	99.72	82.45
24	15	52.04	0.66	2.57	0.14	6.78	0.13	16.32	20.56	0.26	0.01	99.47	81.09
25	20	51.98	0.67	2.46	0.13	6.57	0.14	16.17	20.93	0.29	0.00	99.34	81.43
26	25	51.66	0.74	2.47	0.13	7.97	0.19	16.00	20.09	0.34	0.01	99.58	78.15
27	33	51.62	0.71	2.77	0.21	6.90	0.21	16.12	20.64	0.26	0.00	99.43	80.63
28	41	51.62	0.82	2.47	0.06	8.21	0.18	15.70	19.54	0.32	0.01	98.93	77.31
29	1	50.93	0.80	2.72	0.11	9.40	0.27	16.18	19.21	0.32	0.00	99.94	75.41
30	6	51.22	0.65	2.02	0.13	11.01	0.37	14.58	19.62	0.32	0.00	99.93	70.24
31	20	50.70	0.72	2.55	0.22	8.84	0.29	16.77	19.25	0.30	0.00	99.64	77.17
32	6	50.57	1.26	3.67	0.52	6.30	0.12	14.83	21.26	0.29	0.00	98.82	80.75
33	5	49.55	1.17	3.60	0.37	6.28	0.11	15.58	21.65	0.30	0.00	98.61	81.55
34	5	49.91	1.11	3.38	0.43	6.18	0.13	15.98	21.64	0.37	0.01	99.14	82.17
35	5	49.57	0.98	3.32	0.50	6.31	0.10	15.51	21.43	0.33	0.01	98.06	81.41
36	5	50.33	0.90	2.89	0.51	6.33	0.13	16.38	21.64	0.39	0.03	99.52	82.18
37	5	48.67	1.99	5.29	0.18	7.87	0.14	13.29	20.46	0.96	0.10	98.95	75.06
38	4	51.61	0.71	2.18	0.85	5.22	0.13	16.46	21.49	0.34	0.00	99.00	84.89
39	3	51.16	0.96	2.72	0.68	5.66	0.11	15.31	21.28	0.25	0.00	98.14	82.82
40	3	50.51	1.22	3.77	0.57	6.00	0.10	15.33	21.42	0.31	0.03	99.27	81.99
41	2	52.53	0.68	2.44	0.35	6.23	0.12	15.71	21.33	0.35	0.00	99.73	81.80
42	1	50.68	1.04	3.22	0.89	5.40	0.11	15.43	22.08	0.35	0.00	99.19	83.58

Note. 1–12, Katun' paleoseamount; 13–31, Kurai paleoseamount (13–22, dikes; 23–31, lavas); 32–42, Agardag ophiolites.

2009; Batanova et al., 1996), Bay of Islands on Newfoundland (Batanova et al., 1998), and ophiolite complexes in the Arctic Urals (Simonov et al., 2000). These clinopyroxenes show a steeply sloping REE pattern and differ from the Kurai paleoseamount melts rich in LREE.

The lava pyroxenes are richer in REE than the dike minerals; their REE content is close to that in MIs. A few samples show a negative Eu anomaly suggesting plagioclase fractionation. The REE patterns of the dike clinopyroxenes lack a Eu anomaly, which evidences that the clinopyroxenes

Table 2. Contents of trace and rare-earth elements (ppm) in clinopyroxenes from rocks of the Kurai paleoseamount

Element	1	2	3	4	5	6	7
Th	0.01	0.01	0.01	0.10	0.01	–	–
Rb	7.3	8.7	8.6	16.0	10.2	–	–
Ba	0.11	0.28	1.03	5.36	0.09	–	–
Sr	11	12	16	24	11	–	–
V	377	387	489	432	356	–	–
La	0.19	0.26	0.48	2.03	0.35	0.02	0.03
Ce	1.18	1.48	2.57	6.73	2.10	0.21	0.16
Nd	2.24	3.01	3.88	9.15	4.26	0.55	0.37
Sm	1.38	1.93	2.40	4.50	2.52	0.32	0.20
Eu	0.48	0.68	0.81	1.10	0.87	0.18	0.13
Gd	1.39	2.78	3.01	6.43	3.88	–	–
Dy	2.39	3.56	4.24	8.34	5.30	1.20	0.51
Er	1.88	2.59	3.22	6.53	3.63	0.84	0.37
Yb	1.60	2.28	3.33	6.16	3.25	0.76	0.40
Y	16.9	19.5	27.6	52.7	27.5	–	–
Zr	9.2	10.2	25.4	47.6	15.8	–	–
Nb	0.06	0.10	0.18	0.75	0.11	–	–
Ta	0.21	0.36	0.40	1.01	0.47	–	–

Note. 1–5, clinopyroxenes from rocks of the Kurai paleoseamount (1–3, dikes; 4, 5, lavas); 6, 7, clinopyroxenes from gabbro-norites of the Troodos ophiolites, Cyprus (6) (Batanova et al., 1996), and the Arctic Urals ophiolites (7) (Simonov et al., 2000).

crystallized earlier than the plagioclase capable for the intense accumulation of Eu (Fig. 4).

In general, the results of clinopyroxene analysis point to the active role of plume magmatic systems in the formation of the Katun' and Kurai paleoseamounts and Agardag ophiolites, which agrees with the compositions of basalts from these reference objects (Dobretsov et al., 2004, 2005; Safonova, 2008; Safonova et al., 2008, 2009).

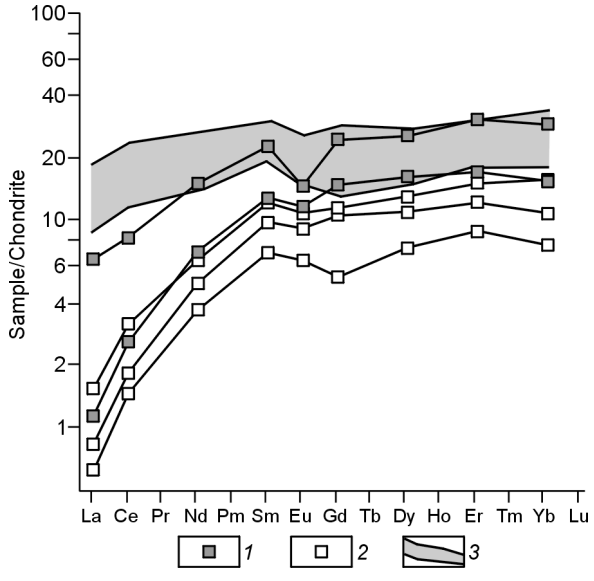

Fig. 4. REE patterns of clinopyroxenes. *1*, *2*, clinopyroxenes from lavas (*1*) and dikes (*2*) from the Kurai paleoseamount; *3*, melt inclusions in these clinopyroxenes.

Clinopyroxene-hosted melt inclusions

Analysis of MIs for each of the studied paleo-oceanic associations was rather specific. For example, it was very difficult to study inclusions in the clinopyroxens from the Katun' paleoseamount and Agardag ophiolites because of their scarcity and small size. Therefore, we obtained poor information on the contents of trace and rare-earth elements; in the case of the Agardag ophiolites, inclusions of the size appropriate for ionic analysis were not found at all. For the Kurai paleoseamount clinopyroxenes, we obtained, on the contrary, a large body of data on MIs. Photomicrographs of the studied MIs are given in Fig. 5, and the results of their analyses, in Tables 3 and 4.

The Katun' paleoseamount. Because of the serious alteration of basaltic rocks, we had to prepare and study many polished plates in order to find MIs. Only 10–15 of >600 examined clinopyroxene grains contained distinctly identified inclusions.

Primary MIs (3–30 μm) are localized in the core of the phenocryst or form bands along the mineral faces. They are rounded, with a slight rectangular faceting, and multiphase: light glass rim + light and dark crystalline phases + ore phases + gas bubble (Fig. 5, *A*). Often, two-phase inclusions with a gas bubble in pure transparent glass occur (Fig. 5, *B*).

Because of the small size of phenocrysts and intense alteration of the groundmass, only a half of the high-temperature experiments with inclusions was successful. During the heating-microstage experiments, primary multiphase MIs in clinopyroxenes and basalts from the Katun' paleoseamount became completely homogeneous within 1130–1170 °C. We

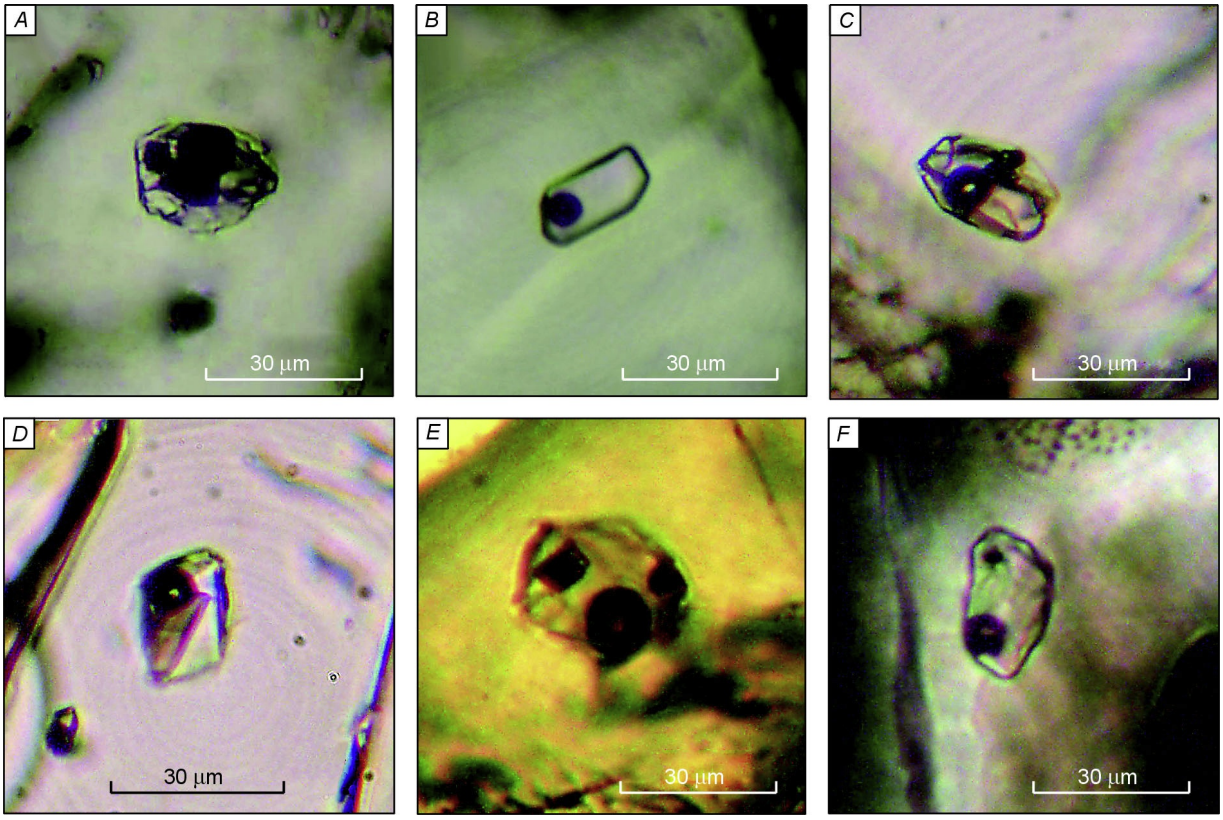

Fig. 5. Photomicrographs of melt inclusions in clinopyroxenes. *A*, *B*, Inclusions in clinopyroxenes from the Katun' paleoseamount rocks; *C*, *D*, inclusions in clinopyroxenes from the Kurai paleoseamount rocks; *E*, *F*, inclusions in clinopyroxenes from the Agardag ophiolite rocks (*F*, heated inclusion).

compared the homogenization temperatures of MI with the liquidus temperatures of their crystallization computed from the data on the MI compositions using the PETROLOG program (Danyushevsky, 2001) and thus estimated the water contents in the melts—0.2 to 0.6 wt.%. We have established that the above temperatures depend directly on the chemical composition of MIs: They grow as the MgO content increases (6.6 wt.% MgO—1140–1145 °C, 9.3 wt.% MgO—1170 °C) and drop as the FeO content decreases. The data for the Katun' paleoseamount partly agree with the data on MIs in the Nauru Basin clinopyroxenes (Fig. 6).

By the proportion of the total content of alkalies, SiO_2 content, and FeO/MgO ratio, the MIs from the Katun' paleoseamount clinopyroxenes fall into the fields of rocks of normal alkalinity and tholeiites. On Harker's variation diagrams, these inclusions are partly of the same composition as the MIs from the Nauru Basin minerals and are generally similar to the MIs in the Kurai paleoseamount clinopyroxenes. As the content of SiO_2 in the melt increases, the contents of TiO_2 and FeO decrease (Fig. 7).

In the TiO_2–FeO/MgO diagram, the MIs from the Katun' paleoseamount pyroxenes are localized in the fields of MORB and within-plate OIB overlapping with the field of the MIs from the Kurai paleoseamount minerals (Fig. 8).

In the TiO_2–K_2O diagram, some composition points of the studied inclusions fall into the fields of MORB and the Ontong Java Plateau basalts and are intimately associated with the inclusions in the Nauru Basin minerals. The rest have high contents of TiO_2 (>2 wt.%) and correspond in composition to within-plate OIB-type plume melts (Fig. 9). The Katun' paleoseamount melts show wide variations in FeO/MgO, thus being similar to the Nauru Basin minerals and differing from MORB, as seen on the Al_2O_3–FeO/MgO diagram (Fig. 10).

In the diagrams of the contents of indicating elements (Nb, Th, Y, Zr, Ti), the composition points of inclusions from the Katun' paleoseamount pyroxenes correspond to melts generated from a plume mantle source and are localized solely in the field of oceanic-plateaubasalts. On the Zr–TiO_2 diagram, the inclusions fall into the field of the Ontong Java Plateau and Nauru Basin basalts and are intimately associated with the MIs from the Nauru Basin pyroxenes (Fig. 11). At the same time, the studied inclusions are similar in the Y–Zr, Nb–Zr, and Zr/Y–Zr correlations to MORB (Fig. 12). The REE patterns of MIs from the Katun' paleoseamount clinopyroxenes are similar to those of the Ontong Java basalts and are identical to those of the Siberian Platform trap basalts, being slightly richer in LREE (Fig. 13).

Modeling by the method of Schilling et al. (1995), based on the MI composition, showed that the primary melts of the Katun' paleoseamount formed at depths of 65–100 km at 1400–1550 °C. These parameters agree with the data on the magmatic systems of the Siberian Platform and the Ontong Java Plateau (Simonov et al., 2005).

Table 3. Representative analyses of homogenized melt inclusions (wt.%)

No.	Run	SiO_2	TiO_2	Al_2O_3	Cr_2O_3	FeO	MnO	MgO	CaO	Na_2O	K_2O	Total	T_{hom}
1	2	49.56	1.47	9.03	0.08	11.48	0.25	10.30	13.87	1.47	0.19	97.70	1140
2	3	49.50	1.51	9.17	0.07	11.55	0.20	9.96	13.79	1.39	0.18	97.32	1140
3	4	49.13	1.46	8.92	0.05	11.46	0.27	10.26	13.84	1.36	0.17	96.92	1140
4	5	49.40	1.46	8.99	0.10	11.56	0.20	9.95	13.68	1.36	0.17	96.87	1140
5	6	49.42	1.41	9.17	0.08	11.20	0.21	10.40	13.83	1.29	0.16	97.17	1140
6	12	49.83	1.69	11.78	0.03	11.38	0.19	8.62	12.30	1.85	0.04	97.71	1170
7	13	50.17	1.73	11.64	0.00	11.18	0.22	8.18	12.18	1.78	0.05	97.13	1170
8	14	51.84	1.74	10.73	0.37	9.01	0.16	10.43	13.11	2.26	0.26	99.90	1170
9	15	51.25	1.82	11.81	0.11	8.83	0.17	8.99	11.82	2.67	0.29	97.76	1170
10	16	50.70	1.83	11.76	0.11	8.83	0.16	8.75	11.76	2.82	0.30	97.02	1170
11	21	48.21	2.10	11.63	0.00	13.79	0.21	6.66	10.64	2.06	0.28	95.58	1145
12	22	48.74	2.10	11.69	0.01	13.88	0.16	6.89	10.60	2.04	0.28	96.39	1145
13	23	48.79	2.22	12.22	0.05	13.71	0.26	6.35	10.60	2.22	0.32	96.74	1145
14	38	49.33	2.11	11.99	0.02	13.05	0.29	6.47	11.17	2.21	0.32	96.95	1140
15	39	49.90	2.18	13.08	0.40	12.97	0.21	6.53	10.95	2.33	0.37	98.92	1140
16	3	49.45	1.87	11.46	0.05	11.46	0.23	8.29	13.01	2.46	0.11	98.39	1180
17	19	49.13	1.94	11.75	0.04	13.01	0.25	7.69	11.70	2.71	0.09	98.31	1175
18	35	49.15	2.01	11.68	0.05	12.91	0.25	7.70	11.65	2.77	0.10	98.27	1170
19	42	47.92	2.16	11.85	0.01	13.74	0.26	8.15	11.69	2.60	0.10	98.48	1175
20	60	47.67	1.94	12.34	0.06	13.08	0.30	8.04	11.91	2.63	0.08	98.05	1165
21	68	51.23	1.35	12.86	0.12	9.57	0.18	8.28	13.53	2.55	0.10	99.77	1180
22	71	47.19	1.68	11.25	0.08	11.79	0.21	9.79	13.44	0.68	0.25	96.37	1170
23	3	51.00	1.61	12.70	0.01	9.83	0.21	7.50	12.45	2.68	0.11	98.08	1190
24	6	49.42	2.17	12.37	0.01	11.72	0.18	7.53	12.45	2.67	0.10	98.61	1190
25	10	47.21	2.53	12.09	0.02	12.59	0.22	8.07	13.24	2.20	0.06	98.23	1165
26	2	50.49	1.70	10.30	0.08	11.15	0.21	9.37	13.67	2.02	0.09	99.09	1180
27	5	49.40	1.97	11.69	0.05	12.98	0.19	7.35	11.68	2.34	0.11	97.77	1180
28	9	49.92	1.55	11.32	0.05	11.32	0.21	8.13	11.95	2.61	0.11	97.17	1170
29	16	53.76	1.07	13.43	0.01	9.87	0.17	6.19	10.83	3.03	0.18	98.54	1155
30	21	52.97	1.17	14.50	0.00	9.80	0.17	5.64	11.08	3.05	0.17	98.54	1160
31	23	47.20	2.60	12.92	0.01	13.20	0.25	7.09	12.20	2.25	0.10	97.81	1160
32	27	51.23	1.96	13.50	0.01	11.77	0.19	5.48	10.26	2.88	0.15	97.44	1165
33	30	49.26	2.29	12.74	0.02	13.80	0.21	5.97	10.24	2.75	0.12	97.41	1165
34	36	52.14	1.64	12.52	0.02	10.66	0.20	6.13	10.69	2.91	0.17	97.08	1170
35	42	50.30	2.17	12.75	0.02	12.32	0.22	6.31	10.24	2.78	0.14	97.26	1155
36	2	50.56	2.01	7.97	0.09	10.49	0.18	10.30	15.06	2.03	0.59	99.27	1230
37	4	49.42	2.31	10.59	0.08	10.32	0.20	8.65	12.44	2.17	0.71	96.89	1210
38	4	49.72	2.31	10.75	0.11	10.25	0.17	8.60	12.22	2.18	0.73	97.03	1210
39	5	49.61	1.77	7.29	0.20	9.77	0.14	10.90	15.84	1.85	0.49	97.86	1245
40	5	49.48	1.71	6.99	0.20	9.83	0.15	11.29	15.81	1.77	0.42	97.66	1255
41	6	48.24	3.07	9.12	0.09	11.76	0.18	9.29	15.49	1.41	0.09	98.74	1230
42	6	48.44	2.88	8.83	0.09	11.58	0.22	9.88	15.94	1.08	0.07	99.01	1230

Note. 1–15, Katun' paleoseamount; 16–35, Kurai paleoseamount (16–25, dikes; 26–35, lavas); 36–42, Agardag ophiolites. T_{hom}, homogenization temperatures of melt inclusions, ℃.

The Kurai paleoseamount. Melt inclusions were studied in clinopyroxenes from porphyrites composing dikes and lava flows. Many original data on MIS were obtained (more than 110 analyses), which were used to determine the parameters of magmatic systems that formed the basaltic complexes of the Kurai paleoseamount.

Primary MIs (5–75 μm) occur uniformly or along straightforward bands in pyroxene crystals. The inclusions are mainly rectangular, sometimes, close to hexagonal, multiphase: round gas bubble + several brownish and greenish crystalline phases + ore phase + light glass (Fig. 5, *C*, *D*).

The homogenization temperatures of MIs from dike rocks and those from lava flows are nearly the same: 1145–1190 ℃ and 1155–1180 ℃, respectively. The calculations of liquidus temperatures from the MI composition using the PETROLOG program (Danyushevsky, 2001) showed that the calculated and

Table 4. Contents of trace and rare-earth elements (ppm) in homogenized melt inclusions

Element	1	2	3	4	5	6	7	8	9	10	11	12	13
Th	0.36	0.10	0.13	0.18	0.14	0.10	0.17	0.17	0.14	0.20	0.18	0.11	0.18
Rb	13	12	14	15	14	13	13	10	14	13	16	13	15
Ba	37	9	10	12	13	8	15	16	12	12	16	6	15
Sr	127	102	123	132	123	87	136	147	112	127	138	51	85
V	291	401	485	410	394	459	292	172	353	366	452	312	419
La	5.94	2.79	3.80	4.39	4.31	2.72	4.95	3.48	4.06	3.70	6.05	2.72	4.64
Ce	16.23	10.28	13.35	15.20	13.45	10.03	14.74	11.52	13.46	12.51	19.44	12.42	14.84
Nd	10.96	8.67	12.76	14.17	12.46	8.61	13.43	10.21	13.28	12.78	15.42	16.34	15.24
Sm	3.08	3.79	5.11	5.32	4.74	3.83	4.34	3.83	4.75	4.29	4.94	8.17	5.97
Eu	1.13	1.06	1.63	1.87	1.52	1.13	1.58	1.22	1.60	1.49	1.96	1.61	1.71
Gd	2.49	3.36	5.31	6.32	5.42	4.09	5.66	4.92	6.86	5.04	6.72	11.33	7.53
Dy	3.54	4.89	6.75	7.74	6.75	5.17	6.76	5.34	7.44	6.35	7.23	15.39	9.15
Er	1.91	4.28	5.50	5.90	5.29	4.45	4.81	3.92	5.42	4.77	5.77	11.47	6.66
Yb	1.83	4.10	5.49	5.95	5.11	4.03	4.84	3.83	5.21	4.60	5.36	11.35	7.16
Y	17	34	44	47	41	38	46	33	46	43	47	91	55
Zr	63	85	97	111	101	88	127	120	120	116	132	115	111
Nb	7.2	2.1	2.7	2.9	2.5	1.7	3.5	2.6	2.8	2.6	3.6	1.2	3.0
Ta	0.49	0.62	0.91	0.94	0.83	0.62	0.84	0.68	0.95	0.67	1.02	1.27	1.35

Note. 1, Katun' paleoseamount; 2–13, Kurai paleoseamount (2–6, dikes; 7–13, lavas).

experimental data are in the best agreement at 1 kbar. Most inclusions show a direct dependence of their homogenization temperatures on the MgO content. As FeO/MgO increases, the crystallization temperature of clinopyroxenes decreases. In general, the composition points of the Kurai paleoseamount melts fall onto the trend of temperatures decreasing from MIs in pyroxenes from the Agardag ophiolites to those in pyroxenes from the Nauru Basin (Ontong Java Plateau) (Fig. 6).

The glasses of homogenized inclusions correspond in composition to basalts and belong to tholeiitic series. In the $(Na_2O + K_2O)/SiO_2$ ratio the MIs in the Kurai paleoseamount clinopyroxenes are close to those in the clinopyroxenes from the Nauru Basin basalts. As seen from Harker's variation diagrams, the increase in the content of SiO_2 in MIs is accompanied by a decrease in the contents of TiO_2, FeO, MgO, and CaO. On all diagrams, the data on the MIs from the Kurai paleoseamount clinopyroxenes agree with those on the MIs from the Nauru Basin basalts (Fig. 7).

On the TiO_2–FeO/MgO diagram, the MIs from the Kurai paleoseamount porphyrites are characterized by high contents of TiO_2 and wide variations in FeO/MgO, and their composition points fall mainly into the fields of three types of basalts: MORB, OIB, and Ontong Java Plateau basalts (OJB). Most of them are localized in the fields of the Ontong Java Plateau and Nauru Basin. In the prevailing FeO/MgO ratios and TiO_2 contents in the MIs the magmatic systems of the Kurai paleoseamount are similar to the melts of the Ontong Java Plateau and Nauru Basin and are intermediate in characteristics between OIB and OJB (Fig. 8).

The MIs in the Kurai paleoseamount clinopyroxenes are poor in K_2O (0.28 wt.%). Most of them fall into the fields of the Nauru Basin melts and OJB, others are associated with MORB, and the rest are localized in the OIB field (Fig. 9). Obvious differences of the magmatic systems of the Kurai paleoseamount from the MOR ones are well seen on the Al_2O_3–FeO/MgO diagram. The studied MIs, like the Nauru Basin melts, are arranged mainly along the trend of olivine

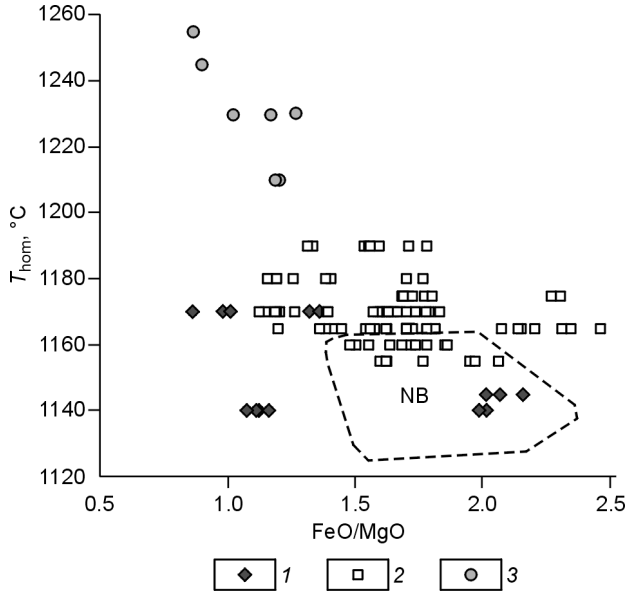

Fig. 6. T_{hom}, °C–FeO/MgO diagram for melt inclusions in clinopyroxenes. *1–3*, melt inclusions in clinopyroxenes from the rocks of the Katun' (*1*) and Kurai (*2*) paleoseamounts and Agardag ophiolites (*3*). Constructed on the basis of our new and earlier (Simonov et al., 2005) data.

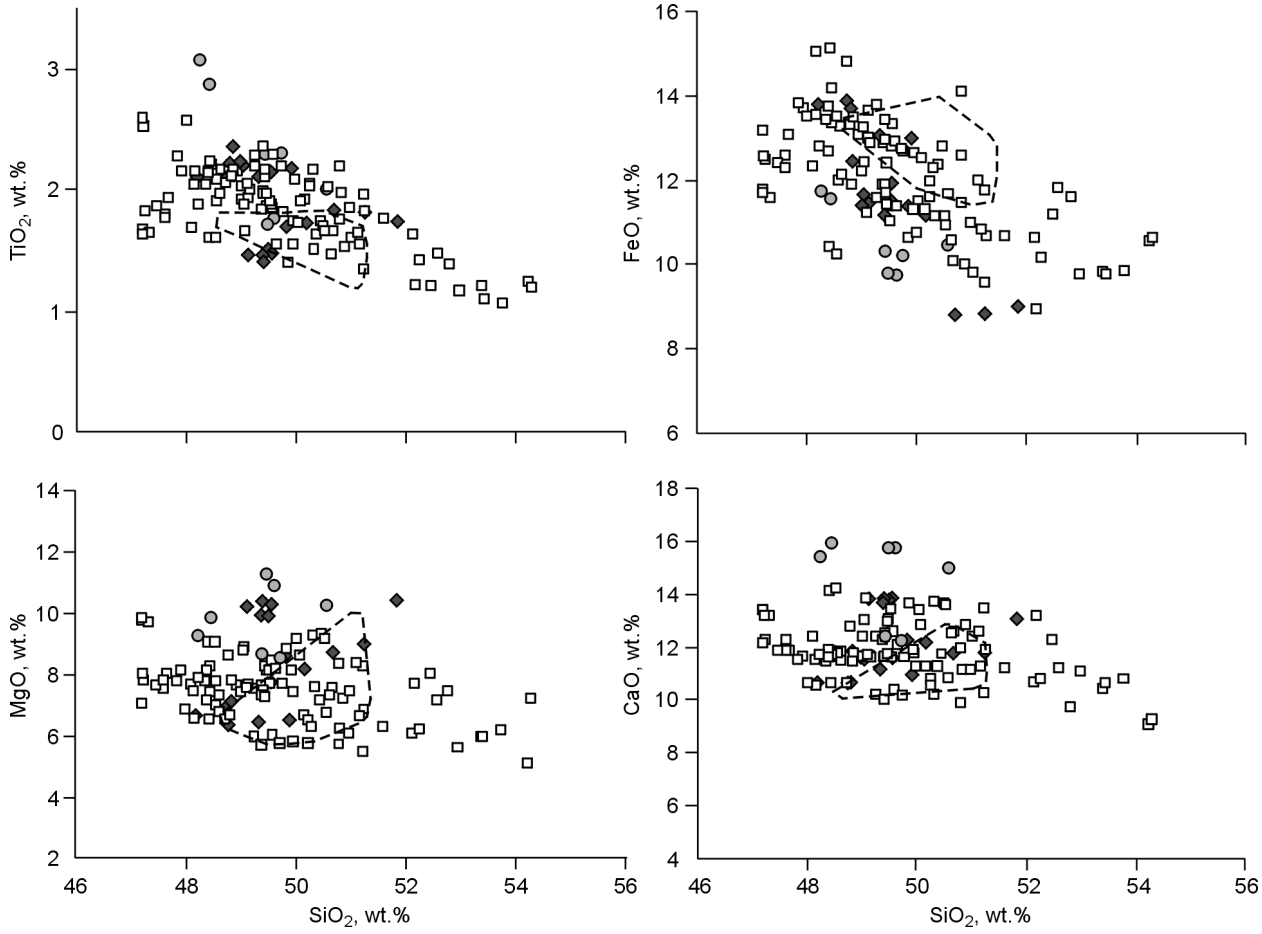

Fig. 7. Harker's diagram for melt inclusions in clinopyroxenes. Dashed line outlines the field of melt inclusions in clinopyroxenes from the Nauru Basin basalts (Ontong Java Plateau). Constructed on the basis of our new and earlier (Simonov et al., 2005) data. Designations follow Fig. 6.

cumulates, whereas MORB are characterized by the minimum FeO/MgO ratios and are localized along the trend of plagioclase cumulates (the contents of Al_2O_3 and FeO are in negative correlation) (Fig. 10).

On the Zr–TiO_2 diagram, the MIs from the Kurai paleoseamount clinopyroxenes are intimately associated with the OJB field (and partly fall into it) (Fig. 11). On the Y–Zr diagram, these MIs, along with glasses and the MIs from the Nauru Basin minerals, are localized along the trend of the Pacific plateaubasalts, differing significantly from both MORB and OIB, which are characterized by more gentle trends of increasing Zr content (Fig. 12). The Kurai paleoseamount MIs show nearly the same REE patterns as the Nauru Basin ones and are associated with the OJB field. They are poorer in LREE than OIB and thus are similar to N-MORB (Fig. 14).

Ion microprobing of the inclusions showed a minor content of water in the Kurai paleoseamount melts (0.04–0.31 wt.%), close to that of the Nauru Basin magmas (0.07–0.18) (Simonov et al., 2004). The MIs are divided into two groups: with low (0.13%) and somewhat higher (0.23–0.31%), typical of N-MORB, H_2O contents. In the H_2O–K and H_2O–Ce correlations the Kurai paleoseamount melts differ from the magmatic systems of MORB and OIB.

Modeling by the method of Schilling et al. (1995), based on the MI composition, showed that the primary magmas of the Kurai paleoseamount formed from two mantle sources localized at depths of 50–65 km (1350–1400 °C) and 65–85 km (1440–1490 °C). The latter parameters are close to those of the magmatic systems in the Nauru Basin (70–110 km, 1440–1500 °C) (Simonov et al., 2004), and the former, to the parameters of the primary melts in MORs (Schilling et al., 1995; Simonov et al., 1999).

The Agardag ophiolites. Primary MIs (5–30 μm in size) form bands in the cores of clinopyroxene phenocrysts. The inclusions are often rectangular and multiphase: light glass(?) + light and dark crystalline phases + gas bubble + ore phases (Fig. 5, *E*, *F*). Fine (3–5 μm) inclusions are predominant, which strongly hampers their study.

During the high-temperature experiments, the MIs homogenized at ~1210–1255 °C. These temperatures are higher than those for the MIs in the pyroxenes from the Katun' and Kurai paleoseamounts. We compared the experimental homogenization temperatures of MIs and the liquidus temperatures calculated from the inclusion compositions using the PETROLOG program (Danyushevsky, 2001). For southern Tuva, their values coincide within the accuracy of the used thermometers. This is independent evidence for the validity of

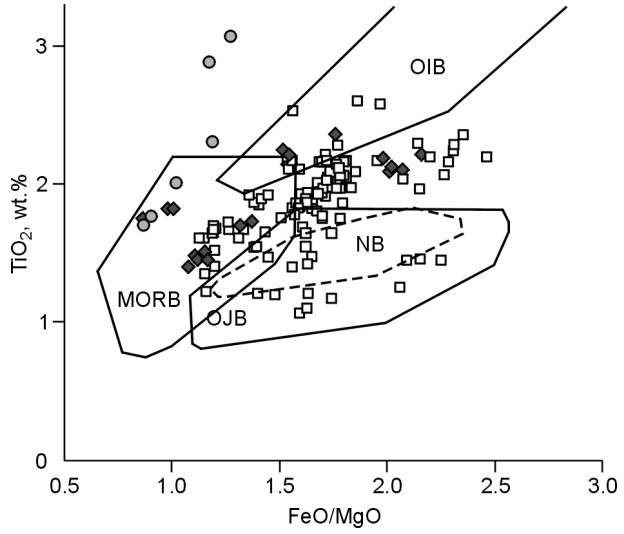

Fig. 8. TiO_2–FeO/MgO diagram for melt inclusions in clinopyroxenes. Fields of MORB, within-plate OIB, and Ontong Java Plateau basalts (OJB) and field of melt inclusions in clinopyroxenes from the Nauru Basin basalts (NB) are shown. Constructed on the basis of our new and earlier (Mahoney et al., 1993; Simonov et al., 1996, 1999, 2005) data. Designations follow Fig. 6.

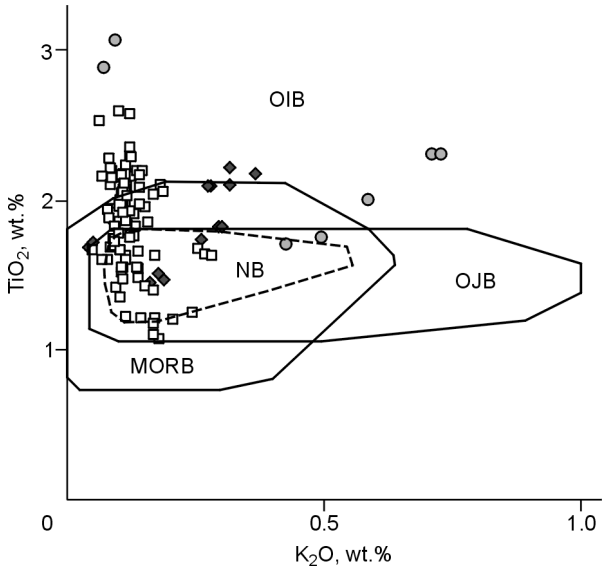

Fig. 9. TiO_2–K_2O diagram for melt inclusions in clinopyroxenes. Designations follow Fig. 8.

the obtained results. We have established a direct dependence of homogenization temperatures of MIs on their composition. An increase in FeO/Mgo is accompanied by a decrease in crystallization temperature from 1255 to 1210 °C (Fig. 6).

By the proportion of total alkalies, FeO/MgO, and SiO_2, the homogenized MIs in clinopyroxene from the Agardag ophiolite lavas are localized in the area of rocks of normal alkalinity, mainly, in the field of tholeiitic rocks, on the Harker diagrams. They show the maximum contents of TiO_2, MgO, and CaO as compared with the MIs in the minerals from the Katun' and Kurai paleoseamounts. The evolution of melts ran with a decrease in TiO_2 and FeO contents. In the contents of almost all elements the studied MIs differ significantly from those from the Nauru Basin basalts (Fig. 7).

On the TiO_2–FeO/MgO diagram, the MIs in the pyroxenes from the Agardag ophiolites form a trend with a drastic

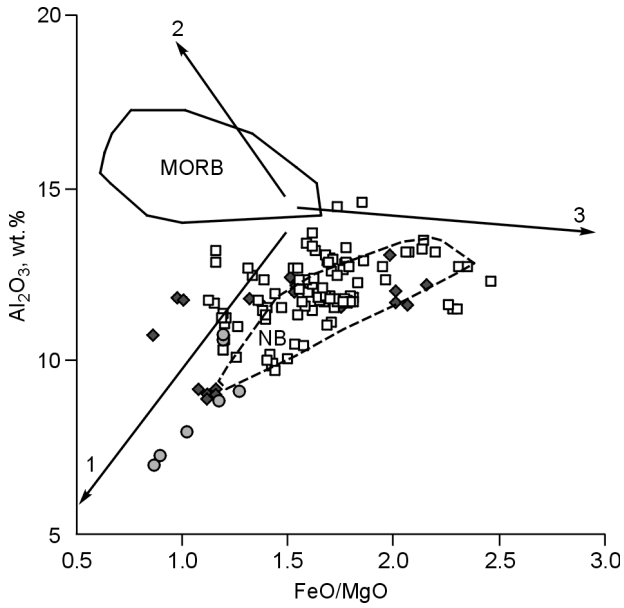

Fig. 10. Al_2O_3–FeO/MgO diagram for melt inclusions in clinopyroxenes. Trends of: 1, olivine cumulates; 2, plagioclase cumulates; 3 ,residual melts. Constructed on the basis of our new and earlier (Simonov et al., 1999, 2005) data. Designations follow Fig. 8.

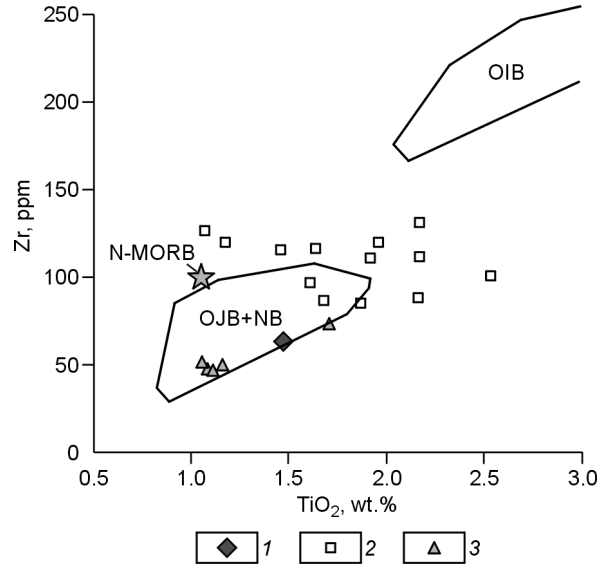

Fig. 11. Zr–TiO_2 diagram for melt inclusions in clinopyroxenes. *1*, *2*, melt inclusions in clinopyroxenes from the rocks of the Katun' (*1*) and Kurai (*2*) paleoseamounts; *3*, basaltic glasses and melt inclusions in clinopyroxenes from the Nauru Basin basalts. Fields of OJB, NB, and OIB are shown. Average data for MORB are given. Constructed on the basis of our new and earlier (Mahoney et al., 1993; Simonov et al., 2000, 2004; Zolotukhin et al., 2003) data.

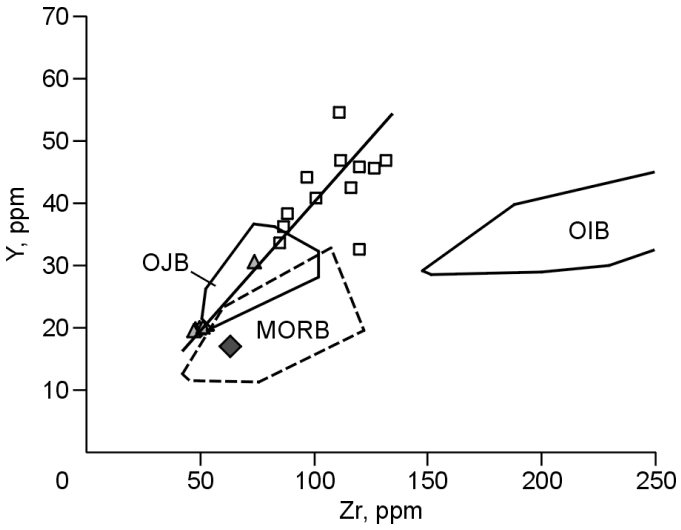

Fig. 12. Y–Zr diagram for melt inclusions in clinopyroxenes. Constructed on the basis of our new and earlier (Mahoney et al., 1993; Simonov et al., 1999, 2005) data. Designations follow Fig. 11.

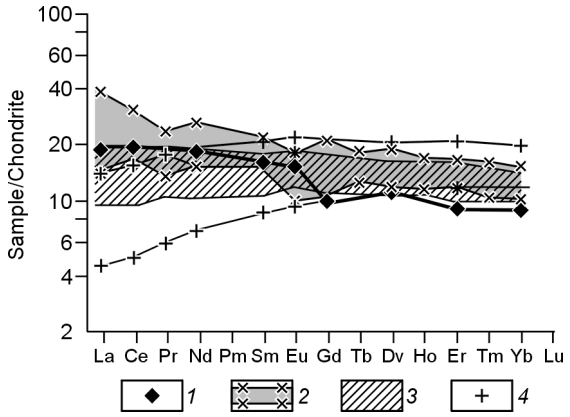

Fig. 13. Chondrite-normalized (Boynton, 1984) REE patterns of melt inclusions. *1*, inclusion in clinopyroxene from the Katun' paleoseamount basalt; *2–4*, fields of basalts: from the Siberian Platform (*2*), from the Ontong Java Plateau (*3*), and N-MORB (*4*). Constructed on the basis of our new and earlier (Mahoney et al., 1993; Sharas'kin, 1992; Simonov et al., 2005) data.

increase in TiO_2 content (up to 3.07 wt.%) and the minimum FeO/MgO value (1.27), which differs them from the MIs from the Katun' and Kurai paleoseamounts (Fig. 8). In the TiO_2–K_2O correlation the inclusions are similar to OIB (Fig. 9). Having the lowest Al_2O_3 contents and FeO/MgO values, they are localized on the trend of olivine cumulates (Fig. 10).

Modeling by the method of Schilling et al. (1995), based on the MI composition, showed that the primary melts of the Tes-Khem site formed mainly at depths of 45–90 km at 1330–1500 ℃.

Conclusions

Our study of clinopyroxenes and their hosted melt inclusions allowed us to estimate the physico-chemical parameters

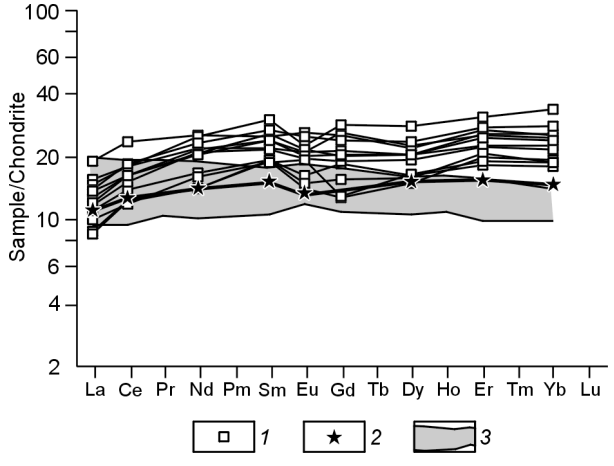

Fig. 14. Chondrite-normalized (Boynton, 1984) REE patterns of melt inclusions. *1*, *2*, inclusions in clinopyroxenes from the basalts of the Kurai plaeoseamount (*1*) and Nauru Basin (*2*); *3*, field of the Ontong Java Plateau basalts. Constructed on the basis of our new and earlier (Mahoney et al., 1993; Simonov et al., 2005) data.

of plume-related magmatic systems, which were active in the Paleo-Asian Ocean during the Neoproterozoic and Early Cambrian.

1. The compositions of clinopyroxenes from the Katun paleoseamount are indicative of the interaction of plume-related and mid-oceanic ridge magmatic systems. The Kurai paleoseamount is characterized by plateaubasalt-type magmatic systems, and the Agardag ophiolites were formed in relation to the OIB-type within-plate magmatism of "hot spots".

2. The analysis of inclusions showed that the melts, which produced the Katun' and Kurai paleoseamounts, crystallized at 1130–1190 ℃, i.e., close to the temperatures typical of plateaubasalt formation, but below those estimated for the Agardag ophiolites (1210–1255 ℃).

3. The Katun' and Kurai melt inclusions are compositionally characterized by lower Mg and Ti compared to the Agardag ophiolites: the former possess chemical affinities with the Nauru Basin and Ontong Java Plateau basalts and the latter—with those of OIB-type basalts of "hot spots".

4. The rare-element compositions of Katun' and Kurai melt inclusions are also similar to those of the Nauru Basin and Ontong Java Plateau basalts, however displaying some features similar to those typical of mid-oceanic ridge magmatism.

5. The numerical simulations of the formation of primary melts showed that the Katun' magmas formed at the physico-chemical parameters close to those of the Siberian Platform and Ontong Java plateau basalts. The Kurai basalts resulted from the interaction of plume-related and mid-oceanic ridge magmatic systems, which is typical of the Nauru Basin and Ontong Java Plateau basalts. The Agardag ophiolites were influenced by plume-related mantle sources melted at initial stages of formation of paleo-oceanic units.

6. In summary, our performed study of clinorypoxenes and their hosted melt inclusions showed that the basaltic units of the Katun' and Kurai paleoseamounts were formed in within-

plate settings of the Paleo-Asian Ocean as a result of the interaction of plateaubasalt-type melts with mid-oceanic ridge magmatic units.

The Teskhem dikes and lavas of the Agardag ophiolites are geochemically similar to the Tihama-Azir dike complex of the Red Sea Region and also to abnormal plume basalts of the Woodlark basin (Pacific Ocean). Based on the obtained data on the pyroxenes and melt inclusions we suggest that the Agardag Ophiolites were formed at the stage of initial plume-induced rifting followed by the opening of spreading basin with oceanic crust at a margin of the Paleo-Asian Ocean.

The mantle plume activity played a crucial role in both cases. But these plumes have characteristic features close to different possible model objects (the Ontong Java Plateau for the Katun' and Kurai paleoseamounts and Red Sea Region with the East African plume for the Agardag ophiolites), considered earlier (Dobretsov, 2008).

This work was supported by the RFBR-JSPS grant 07-05-91211 and Project ONZ 10.1.

References

Batanova, V.G, Savelieva, G.N., 2009. Melt migration in the mantle beneath spreading zones and formation of replacive dunites: a review. Russian Geology and Geophysics (Geologiya i Geofizika) 50 (9), 763–778 (992–1012).

Batanova, V.G., Sobolev, A.V., Schminke, H.U., 1996. Initial melts of intrusive cumulates from the Troodos massif, Cyprus: results of study of clinopyroxenes and melt inclusions in plagioclases. Petrologiya 4 (3), 272–282.

Batanova, V.G., Suhr, G., Sobolev, A.V., 1998. Origin of geochemical heterogeneity in mantle peridotites from the Bay of Islands ophiolite, Newfoundland, Canada: ion probe study of clinopyroxenes. Geochim. Cosmochim. Acta 62 (5), 853–866.

Boynton, W.V., 1984. Geochemistry of the rare earth elements: meteorite studies, in: Henderson, P. (Ed.), Rare Earth Element Geochemistry. Elsevier, Amsterdam, pp. 63–114.

Coleman, R.G., Hadley, D.G., Fleck, R.J., Hedge, K.T., Donato, M.M., 1979. Miocene ophiolites of the Tehama Asir ophiolites and their genesis in relation to the formation of the Red Sea, in: Tectonic Evolution of the Earth's Crust and Faults [in Russian]. Nauka, Moscow, pp. 107–123.

Danyushevsky, L.V., 2001. The effect of small amounts of H_2O on crystallisation of mid-ocean ridge and backarc basin magmas. J. Volcan. Geoth. Res. 110 (3–4), 265–280.

Dobretsov, N.L., 2003. Evolution of structures of the Urals, Kazakhstan, Tien Shan, and Altai–Sayan region within the Ural–Mongolian fold belt (Paleoasian ocean). Geologiya i Geofizika (Russian Geology and Geophysics), 44 (1–2), 5–27 (3–26).

Dobretsov, N.L., 2008. Geological implications of the thermochemical plume model. Russian Geology and Geophysics (Geologiya i Geofizika) 49 (7), 441–454 (587–604).

Dobretsov, N.L., Buslov, M.M., Safonova, I.Yu., Kokh, D.A., 2004. Fragments of oceanic islands in the Kurai and Katun' accretionary wedges of Gorny Altai. Geologiya i Geofizika (Russian Geology and Geophysics) 45 (12), 1381–1403 (1325–1348).

Dobretsov, N.L., Simonov, V.A., Buslov, M.M., Kotlyarov, A.V., 2005. Magmatism and geodynamics of the Paleoasian ocean at the Vendian–Cambrian stage of its evolution. Russian Geology and Geophysics (Geologiya i Geofizika) 46 (9), 933–951 (952–967).

Gibsher, A.S., Terleev, A.A., 1988. Regional stratigraphy of the Late Precambrian–Early Paleozoic in Sangilen, in: Structure-Lithologic Complexes in Southeastern Tuva [in Russian]. IGiG SO AN SSSR, Novosibirsk, pp. 3–26.

Gordienko, I.V., Filimonov, A.V., 2005. The Dzhida zone of the Paleo-Asian ocean: structure and main stages of geodynamic evolution, in: The Geodynamic Evolution of Lithosphere of the Central Asian Mobile Belt (from Ocean to Continent) [in Russian]. Institut Zemnoi Kory SO RAN, Irkutsk, pp. 63–66.

Gordienko, I.V., Mikhal'tsov, N.E., Filimonov, A.V., 2003. Composition and structural position of the Upper Devonian Urmin sequence in the folded framing of the southern Siberian Platform: evidence from paleomagnetic data. Dokl. Earth Sci. 389 (2), 149–153.

Gordienko, I.V., Filimonov, A.V., Minina, O.R., Gornova, M.A., Medvedev, A.Ya., Klimuk, V.S., Elbaev, A.L., Tomurtogoo, O., 2007. Dzhida island-arc system in the Paleoasian Ocean: structure and main stages of Vendian–Paleozoic geodynamic evolution. Russian Geology and Geophysics (Geologiya i Geofizika) 48 (1), 91–106 (120–140).

Izokh, A.E., Vladimirov, A.G., Stupakov, S.I., 1988. Magmatism in the Agardag suture zone (southeastern Tuva), in: Geological and Petrological Research in Southeastern Tuva [in Russian]. IGiG SO AN SSSR, Novosibirsk, pp. 19–75.

Kozakov, I.K., Kovach, V.P., Yarmolyuk, V.V., Kotov, A.B., Sal'nikova, E.B., Zagornaya, N.Yu., 2003. Crust-forming processes in the geologic evolution of the Tuva–Mongolian massif: Sm-Nd isotope and geochemical data on granitoids. Petrologiya 11 (5), 491–511.

Mahoney, J.J., Storey, M., Duncan, R.A., Spencer, K.J., Pringle, M., 1993. Geochemistry and geochronology of Leg 130 basement lavas: nature and origin of the Ontong Java Plateau. Proceedings of the Ocean Drilling Program, Scientific Results 130, 3–22.

Pallister, J.A., Knight, R.J., 1981. Rare earth element geochemistry of Samail ophiolite near Ibrea, Oman. J. Geoph. Res. 86, 2673–2697.

Safonova, I.Yu., 2008. Geochemical evolution of within-plate oceanic magmatism in the Paleo-Asian ocean from Late Proterozoic to Early Cambrian. Petrologiya 16 (5), 527–547.

Safonova, I.Yu., 2009. Intra-plate magmatism and Oceanic Plate Stratigraphy of the Paleo-Asian and Paleo-Pacific oceans. Ore Geol. Rev. 35, 137–154.

Safonova, I.Yu., Buslov, M.M., Iwata, K., Kokh, D.A., 2004. Fragments of Vendian–Early Carboniferous oceanic crust of the Paleo-Asian Ocean in foldbelts of the Altai–Sayan region of Central Asia: geochemistry, biostratigraphy and structural setting. Gondwana Res. 7, 771–790.

Safonova, I.Yu., Simonov, V.A., Buslov, M.M., Ota, T., Maruyama, Sh., 2008. Neoproterozoic basalts of the Paleo-Asian Ocean (Kurai accretionary zone, Gorny Altai, Russia): geochemistry, petrogenesis, and geodynamics. Russian Geology and Geophysics (Geologiya i Geofizika) 49 (4), 254–271 (335–356).

Safonova, I.Yu., Utsunomiya, A., Kojima, S., Nakae, S., Koizumi, K., Tomurtogoo, O., Filippov, A.N., 2009. Pacific superplume-related oceanic basalts hosted by accretionary complexes of Central Asia, Russian Far East and Japan. Gondwana Res., doi: 10.1016/j.gr.2009.02.008.

Schilling, J.-G., Ruppel, C., Davis, A.N., McCully, B., Tighe, S.A., Kingsley, R.H., Lin, J., 1995. Thermal structure of the mantle beneath the equatorial Mid-Atlantic Ridge: influences from the spatial variation of dredged basalt glass compositions. J. Geophys. Res. 100 (B7), 10,057–10,076.

Sharas'kin, A.Ya., 1992. Tectonics and Magmatism of Marginal Seas in Relation to the Problems of the Crust and Mantle Evolution [in Russian]. Nauka, Moscow.

Simonov, V.A., 1993. Petrogenesis of Ophiolites (Thermobarogeochemical Studies) [in Russian]. OIGGM SO RAN, Novosibirsk.

Simonov, V.A., Kolobov, V.Yu., Kovyazin, S.V., 1996. Petrochemical features of basalt magmas in the vicinity of the Bouvet Triple Junction (South Atlantic). Geologiya i Geofizika (Russian Geology and Geophysics) 37 (2), 86–96 (78–87).

Simonov, V.A., Kolobov, V.Yu., Peive, A.A., 1999. Petrology and Geochemistry of Geodynamic Processes in the Central Atlantic Region [in Russian]. Izd. SO RAN, NITs OIGGM, Novosibirsk.

Simonov, V.A., Lesnov, F.P., Stupakov, S.I., 2000. Geochemistry of rare-earth and trace elements in clinopyroxenes from the rocks of the Voikar-Syn'ya and Khadata ophiolite complexes (Arctic Urals), in: Petrology of Igneous and Metamorphic Complexes [in Russian]. TGU, Tomsk, pp. 65–69.

Simonov, V.A., Zolotukhin, V.V., Kovyazin, S.V., Al'mukhamedov, A.I., Medvedev, A.Ya., 2004. Petrogenesis of basaltic series of the underwater

Ontong Java Plateau and Nauru Basin, Pacific. Petrologiya 12 (2), 191–203.

Simonov, V.A., Kovyazin, S.V., Vasil'ev, Yu.R., Mahoney, J., 2005. Physicochemical parameters of continental and ocanic plateau-basalt magmatic systems (from data on melt inclusions). Russian Geology and Geophysics (Geologiya i Geofizika) 46 (9), 886–903 (908–923).

Simonov, V.A., Safonova, I.Yu., Kovyazin, S.V., 2008. Physicochemical parameters of magmatic systems of the Katun' paleoseamount (Paleo-Asian ocean), in: Geodynamic Evolution of the Lithosphere of the Central Asian Mobile Belt (from Ocean to Continent) [in Russian]. Institut Zemnoi Kory SO RAN, Irkutsk, Vol. 2, pp. 96–97.

Sobolev, A.V., 1996. Melt inclusions in minerals as a source of important petrological information. Petrologiya 4 (3), 228–239.

Sobolev, A.V., Danyushevsky, L.V., 1994. Petrology and geochemistry of boninites from the north termination of the Tonga Trench: constraints on the generation conditions of primary high-Ca boninite magmas. J. Petrol. 35, 1183–1211.

Sobolev, A.V., Slutskii, A.B., 1984. Composition and crystallization conditions of the initial melt of the Siberian meimechites in relation to the general problem of ultrabasic magmas. Geologiya i Geofizika (Russian Geology and Geophysics) 25 (12), 97–110 (93–104).

Sobolev, A.V., Sobolev, S.V., Kuzmin, D.V., Malitch, K.N., Petrunin, A.G., 2009. Siberian meimechites: origin and relation to flood basalts and kimberlites, Russian Geology and Geophysics (Geologiya i Geofizika) 50 (12), 999–1033 (1293–1334).

Tarasko, D.A., Kotlyarov, A.V., Simonov, V.A., 2005. The structure of the Tes-Khem site of the Agardag zone in southern Tuva: data of distant sounding, in: Metallogeny of Ancient and Modern Oceans, 2005. Proc. 11th Sci. Student School [in Russian]. IMin UrO RAN, Miass, pp. 163–164.

Tsameryan, O.P., Sobolev, A.V., Zakariadze, G.S., 1991. Application of data on mineralogy of phenocrysts for typification of ophiolite volcanic series of the Little Caucasus. Geokhimiya, No. 11, 1561–1572.

Uchio, Y., Isozaki, Yu., Ota, T., Utsunomiya, A., Buslov, M., Maruyama, Sh., 2004. The oldest mid-oceanic carbonate buildup complex: setting and lithofacies of the Vendian (Late Neoproterozoic) Baratal limestone in the Gorny Altai Mountains, Siberia. Proceedings of the Japan Academy 80, 422–428.

Zolotukhin, V.V., Simonov, V.A., Al'mukhamedov, A.I., Medvedev, A.Ya., Vasil'ev, Yu.R., 2003. Comparative analysis of continental and oceanic plateau basalts (data on the Siberian Platform and Ontong Java Plateau). Geologiya i Geofizika (Russian Geology and Geophysics) 44 (12), 1339–1348 (1293–1302).